European Radiology (2019) 29:4349–4356
https://doi.org/10.1007/s00330-018-5777-4

CARDIAC

Image quality and diagnostic accuracy of coronary CT angiography derived from low-dose dynamic CT myocardial perfusion: a feasibility study with comparison to invasive coronary angiography

Xu Dai[1] · Mengmeng Yu[1] · Jingwei Pan[2] · Zhigang Lu[2] · Chengxing Shen[2] · Yining Wang[3] · Bin Lu[4] · Jiayin Zhang[1]

Received: 23 June 2018 / Revised: 27 August 2018 / Accepted: 19 September 2018 / Published online: 9 November 2018

Abstract

Objectives To investigate the diagnostic performance of coronary CT angiography derived from dynamic CT myocardial perfusion imaging ($CCTA_{CT\text{-}MPI}$) by third-generation dual-source CT with reference to invasive coronary angiography (ICA).

Materials and methods Patients with acute myocardial infarction and those who received successful reperfusion treatment were prospectively enrolled. Emergent ICA findings were used as the reference standard to assess the diagnostic performance of $CCTA_{CT\text{-}MPI}$ for detection of significant coronary stenosis (diameter stenosis ≥ 50%). The radiation dose as well as image quality of $CCTA_{CT\text{-}MPI}$ was also assessed.

Results Twenty-six patients with 352 segments were ultimately included for analysis. The mean radiation dose of $CCTA_{CT\text{-}MPI}$ generated from dynamic CT-MPI was 3.2 ± 1.1 mSv. Overall, 93.5% of total segments were interpretable (Likert score 2–4) whereas 6.5% segments were non-diagnostic (Likert score 1). Twenty-two patients with 84 segments were diagnosed by $CCTA_{CT\text{-}MPI}$ as having ≥ 50% stenosis presence, whereas 268 segments had no obstructive stenosis. Compared to ICA findings, the overall diagnostic accuracy of $CCTA_{CT\text{-}MPI}$ of patient-based and vessel-based as well segment-based analysis was 92.3%, 83.6%, and 85.8% respectively. As shown by ROC analysis, the AUC of $CCTA_{CT\text{-}MPI}$ for detection of ≥ 50% stenosis was 0.833 on a per-patient level, 0.843 on a per-vessel level, and 0.822 on a per-segment level.

Conclusions $CCTA_{CT\text{-}MPI}$ derived from dynamic CT-MPI was able to accurately diagnose obstructive coronary stenosis with reference to ICA.

Key Points

- *CCTA derived from dynamic CT-MPI had a diagnostic image quality in 93.5% of total segments.*
- *CCTA derived from dynamic CT-MPI was accurate in diagnosing obstructive CAD compared to ICA.*
- *The mean radiation dose of dynamic CT-MPI for reconstruction of CCTA was 3.2 mSv.*

Keywords Coronary artery disease · Multidetector computed tomography · Angiography · Myocardial perfusion imaging · Percutaneous coronary intervention

Xu Dai and Mengmeng Yu contributed equally to this work.

✉ Jiayin Zhang
andrewssmu@msn.com

[1] Institute of Diagnostic and Interventional Radiology, Shanghai Jiao Tong University Affiliated Sixth People's Hospital, No. 600, Yishan Rd., Shanghai 200233, China

[2] Department of Cardiology, Shanghai Jiao Tong University Affiliated Sixth People's Hospital, No. 600, Yishan Rd., Shanghai, China

[3] Department of Radiology, Peking Union Medical College Hospital, Chinese Academy of Medical Science & Peking Union Medical College, Beijing, China

[4] Department of Radiology, Fuwai Hospital, State Key Laboratory of Cardiovascular Disease, National Centre for Cardiovascular Diseases, Chinese Academy of Medical Sciences and Peking Union Medical College, Beijing, China

Abbreviations

$CCTA_{CT\text{-}MPI}$	Coronary computed tomography angiography derived from CT myocardial perfusion imaging
CNR	Contrast-to-noise ratio
CT	Computed tomography
DS	Diameter stenosis
ICA	Invasive coronary angiography
MPI	Myocardial perfusion imaging
NPV	Negative predictive value
PPV	Positive predictive value
SNR	Signal-to-noise ratio

Introduction

CT myocardial perfusion imaging (CT-MPI) is a non-invasive functional imaging modality that can successfully evaluate hemodynamically significant coronary stenosis compared to single-photon emission computed tomography (SPECT) MPI or invasive fractional flow reserve (FFR) [1–4]. Dynamic CT-MPI provides quantitative parameters, such as myocardial blood flow (MBF) and myocardial blood volume (MFV), which might further improve the diagnostic accuracy [5–7]. Yet, standard CT-MPI protocol includes both stress perfusion and rest coronary CT angiography (CCTA) for functional and anatomical assessment [8]. This combined procedure usually leads to high overall radiation dose throughout the whole examination procedure [9].

With the recent introduction of third-generation dual-source CT, dynamic CT-MPI can be performed with wider coverage and higher temporal resolution [10]. It is technically feasible to generate CCTA images using part of dataset extracted from dynamic perfusion, which is potentially useful to save additional CCTA acquisition and reduce radiation exposure. Nevertheless, the image quality and diagnostic performance of this CT-MPI-derived CCTA ($CCTA_{CT\text{-}MPI}$) has not yet been explored. Therefore, the current study aims to investigate the image quality and diagnostic accuracy of $CCTA_{CT\text{-}MPI}$ with reference to invasive coronary angiography (ICA).

Material and methods

Patient population

The study cohort was selected from a prospective study to investigate the diagnostic performance of dynamic CT-MPI for detection of myocardial infarction (MI) and microvascular obstruction (MVO) with reference to cardiac magnetic resonance (CMR). Between January 2018 and April 2018, patients with ST-segment elevation myocardial infarction (STEMI) and those who received successful reperfusion treatment within 2 weeks were prospectively enrolled from the cardiology service. Inclusion criteria were the following: (1) patients with STEMI confirmed by electrocardiogram and serum biomarkers, and those who successfully underwent percutaneous coronary intervention (PCI) of culprit lesions; (2) patients who were hemodynamically stable. Exclusion criteria were the following: (1) patients who were hemodynamically unstable, (2) patients with contradictions to CMR acquisition, (3) patients who refused to undergo CMR and/or dynamic CT-MPI.

Emergent ICA on the admission day was used as the reference standard to evaluate the diagnostic performance of CCTA derived from low-dose dynamic CT-MPI. All patients read and signed the written informed consent, and the study protocol was approved by the hospital ethics committee.

Dynamic CT-MPI protocol

Dynamic CT-MPI was performed using third-generation dual-source CT (SOMATOM Force, Siemens Healthineers), which was equipped with an integrated circuit detector system (Stellar Infinity, Siemens Healthineers). Calcium score was firstly performed to calculate the calcification burden of each pericardial vessel. The scan range of dynamic CT-MPI was determined based on the calcium score images to cover the whole left ventricle, as well as all coronary arteries. A fixed volume of contrast media (50 ml, Iopamidol, 370 mg iodine/ml, Bayer) was given in a bolus injection at the rate of 6 ml/s in all patients, followed by a 40-ml saline flush by using dual-barrel power injector (Tyco). Dynamic CT-MPI acquisition was preformed 5 s after preforming contrast injection. The end-systolic phase (triggered at 250 ms after the R wave in all patients) was set for the dynamic acquisition by using a shuttle mode technique with a coverage of 10.5 cm for complete imaging of the whole left ventricle. Scans were launched every second or third heart cycle according to patient's heart rate, resulting in a series of 10 to 15 phases acquired over a fixed period of 31 s. The acquisition parameters of dynamic CT-MPI are listed as follows: collimation = 96 × 0.6 mm, tube voltage = 70 kVp, rotation time = 250 ms, effective current = 250 mAs, reconstructed slice thickness = 0.75 mm, and reconstructed slice interval = 0.5 mm.

$CCTA_{CT\text{-}MPI}$ reconstruction and image analysis

The whole dataset of dynamic CT-MPI was reviewed and the phase with best arterial enhancement was manually selected for reconstruction. $CCTA_{CT\text{-}MPI}$ was reconstructed with a smooth kernel (BV 40) and iterative reconstruction technique (ADMIRE, level 3). Consequently, data was transferred to an offline workstation (SyngoVia, Siemens Healthineers) for further analysis.

The image quality was assessed using a 4-point Likert scale: 4 = excellent (absence of artifact), 3 = good (presence

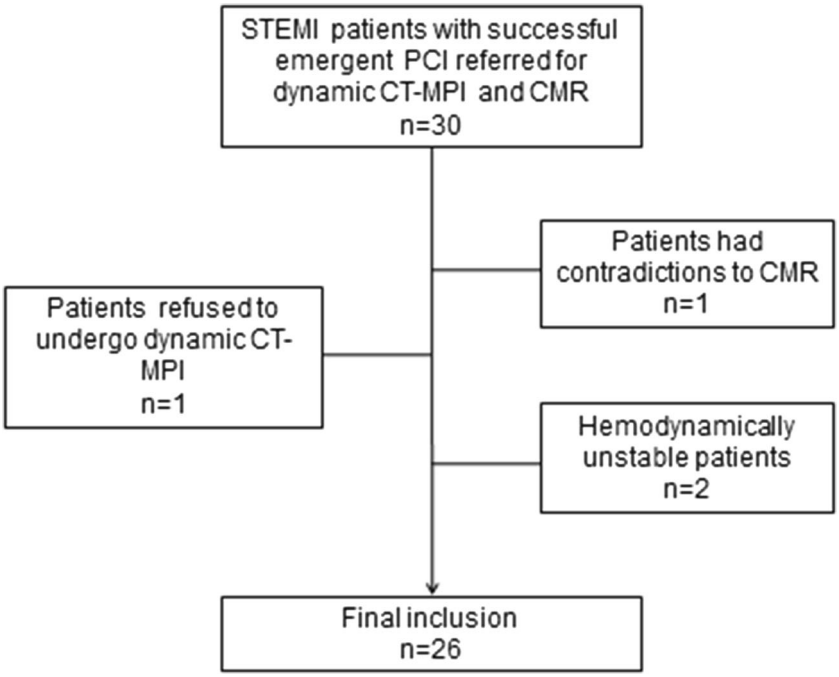

Fig. 1 Flow chart of inclusion and exclusion. CT, computed tomography; CMR, cardiac magnetic resonance; MPI, myocardial perfusion imaging; PCI, percutaneous coronary intervention; STEMI, ST-segment elevation myocardial infarction

of mild artifact), 2 = sufficient (presence of moderate artifact, but still diagnostic), 1 = poor (presence of severe artifact, non-diagnostic). As previously reported [11], various objective image quality parameters, including image noise of the aortic root and proximal coronary arteries, signal-to-noise ratio (SNR), and contrast-to-noise ratio (CNR), were also evaluated. A circular region of interest (ROI) was manually placed in the aortic root at the level of the left main coronary artery ostium (2.5 cm in diameter) to measure lumen attenuation and image noise. The same measurement was also performed

Table 1 Clinical characteristics

Patient number	26
Age (years)	59.5 ± 9.6
Gender	
Females	5 (19.2%)
Males	21 (80.8%)
Weight (kg)	71.4 ± 12.4
BMI	24.9 ± 2.9
Interval between ICA and $CCTA_{CT\text{-}MPI}$ (days)	3.2 ± 1.7
Risk factors	
Hypertension	16 (61.5%)
Hyperlipidemia	6 (23.1%)
Smoking	13 (50.0%)
Diabetes	8 (30.8%)
Agatston score	101.2 ± 141.5 (0.0–507.2)

Abbreviations: *BMI* body mass index, *$CCTA_{CT\text{-}MPI}$* coronary computed tomography angiography derived from CT myocardial perfusion imaging, *ICA* invasive coronary angiography

Table 2 Image quality and radiation dose of $CCTA_{CT\text{-}MPI}$

Heart rate during acquisition (bpm)	78.8 ± 9.4
Volume of contrast medium (ml)	50
Tube voltage (kVp)	70
Radiation dose during CT-MPI acquisition	3.2 ± 1.1
Subjective image quality score (segments)	
1	23 (6.5%)
2	55 (15.6%)
3	98 (27.8%)
4	176 (50.0%)
SNR	
Aorta	14.0 ± 2.8
LM	13.5 ± 2.8
LAD	12.4 ± 3.4
LCx	11.3 ± 4.0
RCA	12.5 ± 2.8
CNR	
Aorta	15.2 ± 2.9
LM	14.4 ± 2.9
LAD	13.1 ± 3.4
LCx	12.2 ± 4.3
RCA	13.3 ± 3.0

Abbreviations: *$CCTA_{CT\text{-}MPI}$* coronary computed tomography angiography derived from CT myocardial perfusion imaging, *CNR* contrast-to-noise ratio, *LAD* left anterior descending, *LCx* left circumflex, *LM* left main, *RCA* right coronary angiography, *SNR* signal-to-noise ratio

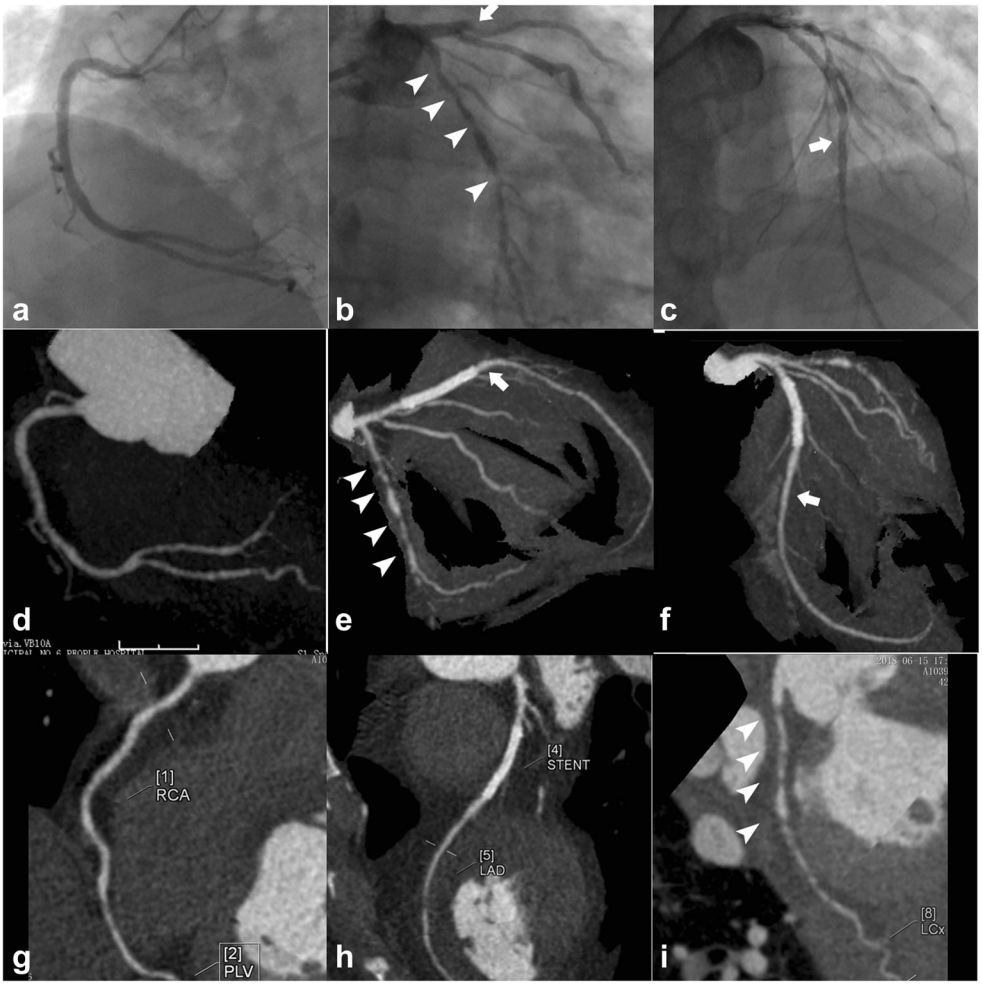

Fig. 2 Representative case of CCTA derived from CT-MPI with comparison to ICA in a 45-year-old male patient of STEMI. **a** Right coronary angiography showed patent RCA. **b** Left coronary angiography showed total occlusion of proximal LAD (white arrow) and multiple severe stenosis of proximal LCx (white arrowhead). **c** Left coronary angiography after PCI revealed restored blood flow of LAD (white arrow). **d** MIP of $CCTA_{CT\text{-}MPI}$ showed patent RCA, which was in accordance with ICA finding. **e**, **f** MIP of $CCTA_{CT\text{-}MPI}$ showed restored flow of LAD (white arrow) and multiple severe stenosis of proximal LCx (white arrowhead), which was also in accordance with ICA finding. **g–i** CPR of $CCTA_{CT\text{-}MPI}$ demonstrated patent RCA and LAD, as well as multiple severe stenosis of proximal LCx (white arrowhead). $CCTA_{CT\text{-}MPI}$, coronary computed tomography angiography derived from CT myocardial perfusion imaging; CT, computed tomography; CPR, curved planar reformation; ICA, invasive coronary angiography; LAD, left anterior descending; LCx, left circumflex; MIP, maximum intensity projection; MPI, myocardial perfusion imaging; PCI, percutaneous coronary intervention; RCA, right coronary angiography; STEMI, ST-segment elevation myocardial infarction

in the proximal segments of the left and right coronary arteries (ROI was drowned as large as possible with exclusion of vessel wall). All ROIs were measured three times, and mean measurements were used for further analysis. The SNR of each measured vessel was calculated by dividing the mean HU by the mean image noise. The proximal vessel contrast was defined as the HU difference between the vessel lumen measurement and the measurement of surrounding tissue immediately next to the vessel contour. The CNR was calculated as the vessel contrast value divided by image noise of the corresponding vessel.

Maximal intensity projection (MIP) and cross-sectional view of coronary arteries were used for evaluation of stenotic extent. The reference diameter was determined as an average of proximal and distal vessel diameter. The minimal lumen diameter (MLD) and proximal/distal vessel diameters were determined as the shortest diameters in eccentric lesions. Diameter stenosis (DS) was defined as (reference diameter − MLD)/reference diameter. The presence of ≥ 50% DS was evaluated on per-patient, per-vessel, and per-segment levels. Obstructive coronary artery disease was considered when DS ≥ 50% was present in at least one segment.

Both image quality and stenosis severity were assessed based on the modified 18-segment classification of the Society of Cardiovascular Computed Tomography [12]. Two cardiovascular radiologists (with 5- and 12-year experience of cardiovascular imaging) who were blinded to the results of

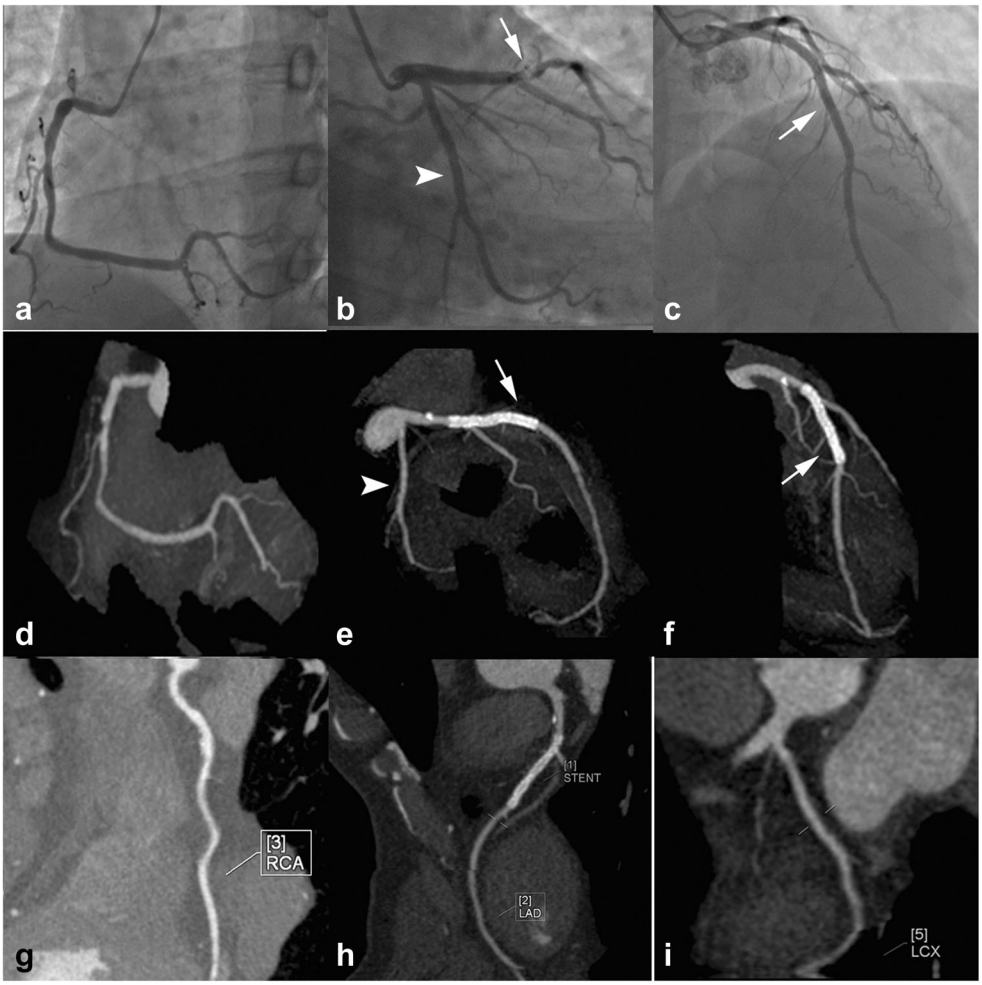

Fig. 3 Representative case of CCTA derived from CT-MPI with comparison to ICA in a 45-year-old male patient of STEMI. **a** Right coronary angiography showed patent RCA. **b** Left coronary angiography showed subtotal occlusion of middle LAD (white arrow) and patent LCx (white arrowhead). **c** Left coronary angiography after PCI revealed restored blood flow of LAD (white arrow). **d** MIP of $CCTA_{CT\text{-}MPI}$ showed patent RCA, which was in accordance with ICA finding. **e**, **f** MIP of $CCTA_{CT\text{-}MPI}$ showed restored flow of LAD (white arrow) and patent LCx (white arrowhead), which was also in accordance with ICA finding. **g–i** CPR of $CCTA_{CT\text{-}MPI}$ demonstrated patent RCA, LAD, and LCx. $CCTA_{CT\text{-}MPI}$, coronary computed tomography angiography derived from CT myocardial perfusion imaging; CT, computed tomography; CPR, curved planar reformation; ICA, invasive coronary angiography; LAD, left anterior descending; LCx, left circumflex; MIP, maximum intensity projection; MPI, myocardial perfusion imaging; PCI, percutaneous coronary intervention; RCA, right coronary angiography; STEMI, ST-segment elevation myocardial infarction

emergent ICA independently evaluated all vessel segments with a diameter of at least 1.5 mm at their origin. For segments with non-diagnostic image quality, they were considered obstructive as non-assessable segments which needed further evaluation by other imaging modalities or ICA in clinical routines to avoid misdiagnosis [13]. Disagreements between the two readers for any image set were resolved by consensus, and the consensus findings were used in all assessments of diagnostic performance.

ICA procedure and analysis

The ICA was performed with standard techniques, and at least two different views were obtained for each main vessel. All segments were evaluated by two interventional cardiologists (with 18- and 24-year experience of coronary intervention). The culprit lesions causing STEMI were determined according to electrocardiogram and ICA findings. PCI was performed to treat culprit lesions and non-culprit lesions were referred for staged PCI. The angiogram post-successful PCI was obtained and used as the reference standard for comparison with $CCTA_{CT\text{-}MPI}$.

Statistical analysis

Statistical analysis was performed using SSPS version 13.0 (SPSS Inc.). One-sample Kolmogorov-Smirnov test was firstly used to check the assumption of normal distribution. Quantitative variables with normal distribution were expressed as mean ± standard deviation (SD), while median

and quartiles were used for variables that were not normally distributed. *T* test and Pearson test were used for data with normal distribution, while Mann-Whitney *U* test was used otherwise. Interobserver agreement was expressed in Cohen's kappa value (*k*) for categorical variables. Sensitivity, specificity, positive predictive value (PPV), and negative predictive value (NPV) were recorded to evaluate the diagnostic performance of $CCTA_{CT\text{-}MPI}$. Using ICA findings as the reference standard, receiver operating characteristic (ROC) curve analysis was performed to calculate the area under the receiver operating characteristic curve (AUC), based on the method developed by Hanley and McNeil [14]. A two-tail probability value of $p < 0.05$ was considered statistically significant.

Results

Clinical characteristics

A total of 30 STEMI patients with successful emergent PCI were initially enrolled. Two hemodynamically unstable patients and one patient having contradictions to CMR were excluded from the study. In addition, one patient who refused to undergo dynamic CT-MPI was further excluded (Fig. 1). Finally, a total of 26 patients were ultimately included in the study (mean age 59.5 ± 9.6 years, range 41 to 75 years, 21 males [mean age 58.5 ± 9.1 years, range 41 to 75] and 5 females [mean age 63.4 ± 11.6 years, range 45 to 75], $p = 0.3159$). ICA was performed with an interval of 3.2 ± 1.7 days (range 1 to 8 days). Detailed demographic data are presented in Table 1.

Image quality and radiation dose of $CCTA_{CT\text{-}MPI}$

The mean dose length product (DLP) of dynamic CT-MPI was 231.3 ± 79.4 mGy × cm (range 100.8 to 432.3 mGy × cm), corresponding to 3.2 ± 1.1 mSv (range 1.41 to 6.05 mSv) when using 0.014 as the conversion factor. Twenty-six patients with 352 coronary segments were finally included for analysis. Overall, 93.5% of total segments were interpretable (Likert score 2–4) whereas 6.5% segments were non-diagnostic (Likert score 1). Notably, the percentage of segments with excellent (Likert score 4) and good (Linkert score 3) image quality was 50% and 27.8%, respectively. The noise level of $CCTA_{CT\text{-}MPI}$ was relatively high (67.3 ± 6.7 in aortic root at the level of the left main coronary artery ostium) while SNR and CNR were acceptable (Table 2).

Diagnostic performance of $CCTA_{CT\text{-}MPI}$ with reference to ICA

Twenty-two patients with 84 segments were diagnosed by $CCTA_{CT\text{-}MPI}$ as having the presence of ≥ 50% DS (Fig. 2), whereas 268 segments revealed no obstructive stenosis (Fig. 3). The interobserver agreement of diagnosing obstructive CAD on a per-patient level by $CCTA_{CT\text{-}MPI}$ was good (kappa = 0.901, $p = 0.02$). Compared to ICA findings, the overall diagnostic accuracy of $CCTA_{CT\text{-}MPI}$ of patient-based and vessel-based as well segment-based analysis were 92.3%, 83.6%, and 85.8% respectively. The diagnostic performance of stenosis assessment was good in terms of sensitivity, specificity, PPV, and NPV (Table 3). As shown by ROC analysis, the AUC for detection of ≥ 50% DS was 0.833 (95% confidence interval [CI], 0.595–1.000) on a per-patient level, 0.843 (95% CI, 0.760–0.926) on a per-vessel level, and 0.822(95% CI, 0.756–0.888) on a per-segment level (Fig. 4).

Discussion

The current study has two main findings: (1) CCTA derived from dynamic CT-MPI is technically feasible and has preserved image quality; (2) $CCTA_{CT\text{-}MPI}$ is accurate for diagnosing the obstructive CAD with reference to ICA.

The standard CT-MPI protocol includes both stress perfusion and rest CCTA acquisition, which results in high radiation exposure. According to one recent review, the average radiation doses of static and dynamic CT-MPI were 5.93 mSv and

Table 3 Diagnostic performance of $CCTA_{CT\text{-}MPI}$ for detection of ≥ 50% diameter stenosis with reference to ICA

Patient-based analysis (*n* = 26)	
Accuracy	92.3% (24/26)
Sensitivity	100% (20/20)
Specificity	66.7% (4/6)
PPV	90.9% (20/22)
NPV	100% (4/4)
Vessel-based analysis (*n* = 104)	
Accuracy	83.6% (87/104)
Sensitivity	86.5% (32/37)
Specificity	82.1% (55/67)
PPV	72.3% (32/44)
NPV	91.7% (55/60)
Segment-based analysis (*n* = 352)	
Accuracy	85.8% (302/352)
Sensitivity	76.7% (46/60)
Specificity	87.7% (256/292)
PPV	54.8% (46/84)
NPV	95.5% (256/268)
Assessable segments	93.5% (329/352)

Abbreviations: *$CCTA_{CT\text{-}MPI}$* coronary computed tomography angiography derived from CT myocardial perfusion imaging, *ICA* invasive coronary angiography, *NPV* negative predictive value, *PPV* positive predictive value

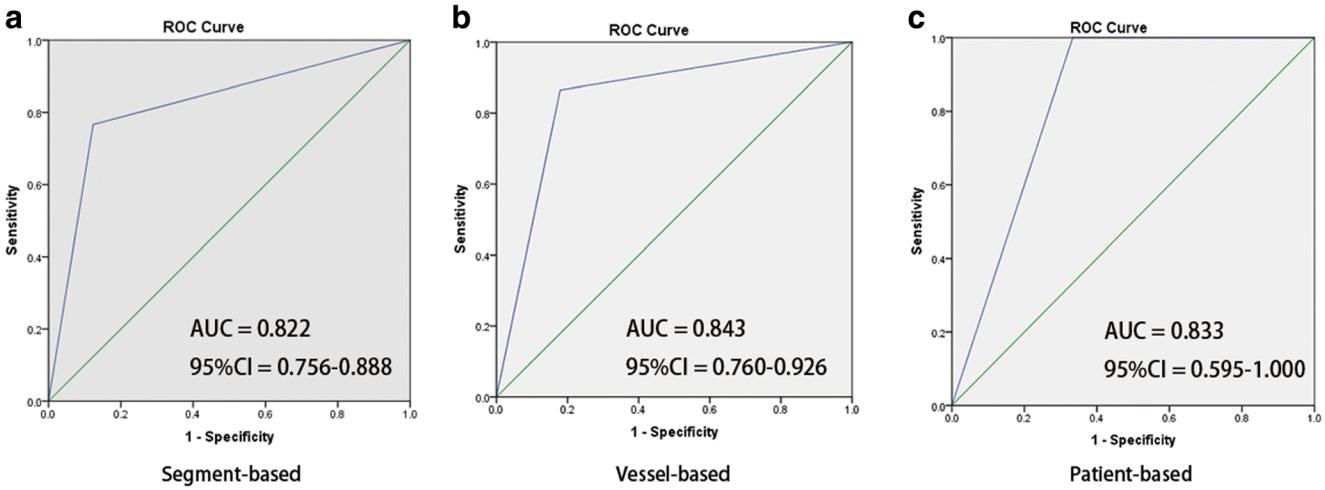

Fig. 4 ROC curve analysis of $CCTA_{CT\text{-}MPI}$ for diagnosing obstructive CAD. **a–c** The segment-based, vessel-based, and patient-based ROC curve analyses of $CCTA_{CT\text{-}MPI}$ for diagnosing obstructive CAD. AUC, area under curve; CAD, coronary artery disease; $CCTA_{CT\text{-}MPI}$, coronary computed tomography angiography derived from CT myocardial perfusion imaging; ROC, receiver operating characteristic

9.23 mSv, respectively [9]. With the introduction of modern dose reduction techniques, the radiation dose of standard low-dose CCTA in different clinical settings is significantly lower compared to CT-MPI [15–19]. The radiation hazard has become a very big disadvantage related to CT-MPI.

To overcome the above shortcoming, we investigated the feasibility of using dynamic CT-MPI dataset to generate CCTA on a third-generation dual-source CT platform. According to the current findings, $CCTA_{CT\text{-}MPI}$ could be successfully reconstructed and the image quality of $CCTA_{CT\text{-}MPI}$ was good and excellent in nearly 80% of total coronary segments. The noise level, SNR, and CNR of $CCTA_{CT\text{-}MPI}$ were slightly inferior to those reported by previous low-dose CCTA study on the same CT platform [11], but still acceptable. This could be ascribed to the recent hardware development of CT scanner with higher temporal and spatial resolution, which leads to less motion artifacts and better image quality. Moreover, using ICA as the reference standard, the diagnostic accuracy of this novel CCTA technique is high on per-segment, per-vessel, and per-patient levels, which could be comparable to the results from previous low-dose CCTA studies [15–17, 20]. In addition, it is reasonable to expect better image quality and diagnostic performance of $CCTA_{CT\text{-}MPI}$ in patients with stable angina or atypical chest pain, who are more compliable than STEMI patients when following scanning instructions such as breath holding. In light of the above promising preliminary results, we might possibly save a dedicated rest CCTA from dynamic CT-MPI and evaluate the coronary anatomy using $CCTA_{CT\text{-}MPI}$. Therefore, the mean radiation dose of CT-MPI protocol could be reduced to around 3.2 mSv as revealed by the present study.

Despite these promising results, the current study has several limitations. Firstly, direct comparison between images from standard CCTA acquisition and from $CCTA_{CT\text{-}MPI}$ was not available because a dedicated CCTA acquisition was not performed in order to reduce the radiation dose as well as contrast medium usage in STEMI patients. Thus, additional studies, including both acquisition protocols, are required to confirm the non-inferiority of $CCTA_{CT\text{-}MPI}$ compared to standard CCTA. Secondly, the present study cohort is patients with myocardial infarction rather than stable angina. The latter one is associated with much higher clinical demands for CT-MPI. Therefore, further studies are needed to validate the current findings in patients with stable angina.

In conclusion, CCTA derived from dynamic CT-MPI is technically feasible and accurate for diagnosis of obstructive CAD with reference to ICA.

Funding This study has received funding from the National Natural Science Foundation of China (Grant No.: 81671678), Shanghai Municipal Education Commission-Gaofeng Clinical Medicine Grant Support (Grant No.: 20161428), Shanghai Key Discipline of Medical Imaging (No.: 2017ZZ02005), and The National Key Research and Development Program of China (Grant No.: 2016YFC1300400, 2016YFC1300402).

Compliance with ethical standards

Guarantor The scientific guarantor of this publication is Dr. Jiayin Zhang.

Conflict of interest The authors of this manuscript declare no relationships with any companies, whose products or services may be related to the subject matter of the article.

Statistics and biometry No complex statistical methods were necessary for this paper.

Informed consent Written informed consent was acquired in all patients.

Ethical approval Institutional Review Board approval was obtained.

Methodology
- Prospective
- Comparative study
- Performed at one institution

References

1. Rochitte CE, George RT, Chen MY et al (2014) Computed tomography angiography and perfusion to assess coronary artery stenosis causing perfusion defects by single photon emission computed tomography: the CORE320 study. Eur Heart J 35(17):1120–1130
2. Ko BS, Cameron JD, Meredith IT et al (2012) Computed tomography stress myocardial perfusion imaging in patients considered for revascularization: a comparison with fractional flow reserve. Eur Heart J 33(1):67–77
3. Ko BS, Cameron JD, Leung M et al (2012) Combined CT coronary angiography and stress myocardial perfusion imaging for hemodynamically significant stenoses in patients with suspected coronary artery disease: a comparison with fractional flow reserve. JACC Cardiovasc Imaging 5(11):1097–1111
4. George RT, Arbab-Zadeh A, Miller JM et al (2012) Computed tomography myocardial perfusion imaging with 320-row detector computed tomography accurately detects myocardial ischemia in patients with obstructive coronary artery disease. Circ Cardiovasc Imaging 5(3):333–340
5. Bamberg F, Becker A, Schwarz F et al (2011) Detection of hemodynamically significant coronary artery stenosis: incremental diagnostic value of dynamic CT-based myocardial perfusion imaging. Radiology 260(3):689–698
6. Schwarz F, Hinkel R, Baloch E et al (2013) Myocardial CT perfusion imaging in a large animal model: comparison of dynamic versus single-phase acquisitions. JACC Cardiovasc Imaging 6(12): 1229–1238
7. Bamberg F, Marcus RP, Becker A et al (2014) Dynamic myocardial CT perfusion imaging for evaluation of myocardial ischemia as determined by MR imaging. JACC Cardiovasc Imaging 7(3): 267–277
8. Rossi A, Merkus D, Klotz E, Mollet N, de Feyter PJ, Krestin GP (2014) Stress myocardial perfusion: imaging with multidetector CT. Radiology 270(1):25–46
9. Danad I, Szymonifka J, Schulman-Marcus J, Min JK (2016) Static and dynamic assessment of myocardial perfusion by computed tomography. Eur Heart J Cardiovasc Imaging 17(8):836–844
10. Pelgrim GJ, Duguay TM, Stijnen JM et al (2017) Analysis of myocardial perfusion parameters in an ex-vivo porcine heart model using third generation dual-source CT. J Cardiovasc Comput Tomogr 11(2):141–147
11. Li Y, Yu M, Li W, Lu Z, Wei M, Zhang J (2018) Third generation dual-source CT enables accurate diagnosis of coronary restenosis in all size stents with low radiation dose and preserved image quality. Eur Radiol 28(6):2647–2654
12. Leipsic J, Abbara S, Achenbach S et al (2018) SCCT guidelines for the interpretation and reporting of coronary CT angiography: a report of the Society of Cardiovascular Computed Tomography Guidelines Committee. J Cardiovasc Comput Tomogr 8(5):342–358
13. Stehli J, Fuchs TA, Bull S et al (2014) Accuracy of coronary CT angiography using a submillisievert fraction of radiation exposure: comparison with invasive coronary angiography. J Am Coll Cardiol 64(8):772–780
14. Hanley JA, McNeil BJ (1982) The meaning and use of the area under a receiver operating characteristic (ROC) curve. Radiology 143(1):29–36
15. Layritz C, Schmid J, Achenbach S et al (2014) Accuracy of prospectively ECG-triggered very low-dose coronary dual-source CT angiography using iterative reconstruction for the detection of coronary artery stenosis: comparison with invasive catheterization. Eur Heart J Cardiovasc Imaging 15(11):1238–1245
16. Yin WH, Lu B, Hou ZH et al (2013) Detection of coronary artery stenosis with sub-milliSievert radiation dose by prospectively ECG-triggered high-pitch spiral CT angiography and iterative reconstruction. Eur Radiol 23(11):2927–2933
17. Meinel FG, Canstein C, Schoepf UJ et al (2014) Image quality and radiation dose of low tube voltage 3rd generation dual-source coronary CT angiography in obese patients: a phantom study. Eur Radiol 24(7):1643–1650
18. Matveeva A, Schmitt RR, Edtinger K et al (2018) Coronary CT angiography in patients with atrial fibrillation: standard-dose and low-dose imaging with a high-resolution whole-heart CT scanner. Eur Radiol 28(8):3432–3440
19. Andreini D, Pontone G, Mushtaq S et al (2018) Image quality and radiation dose of coronary CT angiography performed with whole-heart coverage CT scanner with intra-cycle motion correction algorithm in patients with atrial fibrillation. Eur Radiol 28(4):1383–1392
20. Albrecht MH, Nance JW, Schoepf UJ et al (2018) Diagnostic accuracy of low and high tube voltage coronary CT angiography using an X-ray tube potential-tailored contrast medium injection protocol. Eur Radiol 28(5):2134–2142